0270-6474/82/0210-1387$02.00/0

Printed in U.S.A.

The Journal of Neuroscience
Vol. 2, No. 10, pp. 1387-1404
October 1982

DISCHARGE RATE AND EXCITABILITY OF CORTICALLY PROJECTING INTRALAMINAR THALAMIC NEURONS DURING WAKING AND SLEEP STATES[1]

LOYD L. GLENN AND MIRCEA STERIADE[2]

Laboratoire de Neurophysiologie, Départment de Physiologie, Faculté de Médecine, Université Laval, Québec, Canada G1K 7P4

Received March 31, 1982; Revised June 25, 1982; Accepted June 26, 1982

Abstract

Spontaneous firing and antidromically or synaptically evoked discharges of 89 single neurons in centralis lateralis-paracentralis (CL-Pc) intralaminar thalamic nuclei were examined during waking and sleep states in behaving cats with chronic pontine lesions. Twenty-four neurons were activated synaptically at short latencies from the midbrain reticular formation (MRF) after anterograde degeneration of passing fibers. Sixty-five neurons were identified antidromically as projecting to motor or parietal association cortical areas; of them, 23 also could be excited synaptically from the MRF. These neurons were regarded as possibly being involved in the transfer toward the neocortex of the tonic excitation from the MRF during EEG-desynchronized behavioral states. Rates of spontaneous discharge in CL-Pc neurons doubled from synchronized sleep (S) to either wakefulness (W) or desynchronized sleep (D). First order measures of discharge patterns indicated that interval modes in both W and D states (>10 msec) are significantly different from those in S (2.5 msec). During S, the intervals found in the <5-msec class indicated the intraburst frequencies; a late minor mode (200 to 350 msec) reflected the interburst silent periods. All neurons tested for antidromic activation from cortical areas had enhanced responsiveness in both W and D states as compared to S sleep. In some cases, the enhanced antidromic excitability was observed in conjunction with a transformation from initial segment spikes during S to full spikes in EEG-desynchronized states. During both W and D states, compared to S sleep, the probability of monosynaptically elicited single discharges to MRF stimulation was increased, and the latency and duration of high frequency bursts evoked by MRF volleys were shortened.

We conclude that the features of cortically projecting intralaminar neurons that relay MRF activity fit in well with their hypothesized role in the tonic activation processes that characterize both W and D states. Several lines of evidence suggest that sustained hyperpolarization prevails in intralaminar neurons during S sleep. This is the basic prerequisite for thalamic bursting. The effect of long lasting inhibitory potentials in thalamic neurons provides a mechanism for closing sensory channels during S sleep.

Autoradiography (Edwards and De Olmos, 1976) and electrophysiological studies (Ropert and Steriade, 1981) have disclosed the medial and intralaminar thalamic nuclei to be major rostral targets of the midbrain reticular formation (MRF). In turn, intralaminar nuclei directly project to widespread neocortical areas as shown by retrograde tracing methods (Hendry et al., 1979; Itoh and Mizuno, 1977; Jones and Leavitt, 1974; Kennedy and Baleydier, 1977; Macchi et al., 1977). Electrophysiological investigations of centralis lateralis-paracentralis (CL-Pc) intralaminar thalamic neurons have shown that they are the recipients of monosynaptic excitation from the MRF and that they send axons to pericruciate or anterior suprasylvian cortices of the cat (Steriade and Glenn, 1982). This relay in the CL-Pc nuclei thus could be involved in the transfer of tonic excitation from the reticular formation to the cortex. Such a role would be consistent with the behavior of rostrally projecting MRF neurons during EEG-desynchronized behavioral states (Steriade et al., 1982). The present paper concerns changes, during the sleep-waking cycle, in the sponta-

[1] This work was supported by the Medical Research Council of Canada (Grant MT-3689). Dr. L. L. Glenn was a postdoctoral fellow of the United States National Science Foundation. We are grateful to Mr. G. Oakson for help with the statistical data and to Madame M. Cardinal and Messieurs P. Giguère and D. Drolet for technical assistance.

[2] To whom correspondence and reprint requests should be sent.

neous and evoked discharges of cortically projecting CL-Pc neurons that relay MRF activity. Since EEG synchronization and desynchronization are hypothesized to depend upon thalamic neuronal activity, we wanted to establish (*1*) whether the discharge patterns of intralaminar neurons are similar in the EEG-desynchronized states of wakefulness (W) and desynchronized sleep (D) as opposed to synchronized sleep (S) and (*2*) whether the state-dependent changes in excitability of CL-Pc neurons may adequately account for the cellular correlates of activated and deactivated states found at the cortical level.

Materials and Methods

Preparation. Experiments were conducted on 21 adult cats. The chronic implantation of recording and stimulating electrodes was performed under sodium pentobarbital anesthesia (35 to 40 mg/kg). Recording leads consisted of monopolar surface electrodes for EEGs, silver ball electrodes for ocular movements, and bipolar electrodes for neck EMGs. Bipolar stimulating electrodes with tips bared 0.2 to 0.4 mm were inserted into the MRF (four wires, ≃1.0 mm apart, at coordinates A1 to A4, L2 to L5, D0 to D3) and the deep layers or white matter underlying pericruciate and anterior suprasylvian gyri (arrays of six to eight wires in each region). In a few experiments, we implanted electrodes in the internal capsule midway between CL-Pc nuclei and the pericruciate cortex. The calvarium overlying the microelectrode targets (A7 to A12, L1 to L4) was removed and replaced with a plate. Four fixation cylinders were anchored to the bone with screws and dental cement; during recording sessions, bars were inserted into the cylinders to permit the head to be restrained rigidly in a stereotaxic position without pain or pressure. In order to reduce the likelihood that MRF-evoked responses arise from the stimulation of the fibers of spinothalamic projections or those arising in bulbopontine reticular fields and extrareticular aggregates, the ipsilateral rostral pontine tegmentum was destroyed completely by electrolytic lesions located just caudal to the MRF stimulating electrodes; 10 to 20 days were allotted for the anterograde degeneration of ascending fibers (see Fig. 1*B* in Steriade and Glenn, 1982). Postoperatively, the animals received 150,000 units of penicillin per day for 3 days. The cats required assistance with feeding for 4 to 5 postoperative days.

Recording. Recording sessions began 10 to 20 days after the stimulating electrodes were implanted and the pontine tegmentum was lesioned. The animals slept *ad libitum* between recording sessions. During experiments, the cats were in a sphinx position with their head restrained. They could move their limbs and make postural adjustments in the apparatus. Tungsten microelectrodes (1- to 2-μm tip diameter, 2 to 8 megohms at 1 kHz) pierced the intact dura after removal of the plate. Six to 10 descents ipsilateral to the MRF and cortical electrodes and directed toward the CL-Pc intralaminar nuclei were made in each animal. At the end of each penetration, small lesions (10 to 20 μA, 25 sec) were made at the top and bottom of the track. Only neurons found within the histological borders of CL-Pc are reported in this paper. Figure 1 shows the location of 28 neurons which were found between anterior planes 9 and 10 and could be analyzed statistically (see Appendixes 1 and 2).

Neurons with signs of injury and presumed fibers (exclusively positive discharges with a duration of <0.8 msec) were disregarded. Microelectrode advancement was concurrent with alternating MRF and cortical searching stimuli (0.05 to 0.2 msec in duration). The intensity was set at 0.7 mA during penetration of the electrode. Once a cell was encountered, the current was adjusted to the minimum required to elicit antidromic or synaptic responses, which was usually 0.05 to 0.2 mA. We never stimulated above the threshold for overt movements. There was no behavioral sign that the electrical stimulation was experienced or that the sleep-waking cycle was disturbed by such stimuli. The unilateral pontine lesions did not change the sequence of the sleep-waking cycle; quantitative measurements of the amounts of wake and sleep states have not been made.

The procedure that we used follows. First, all MRF and cortical testing stimuli were checked for responses; this paper is based exclusively on CL-Pc neurons that were invaded antidromically from pericruciate or anterior suprasylvian areas and/or driven synaptically from the MRF. After identification, we tested the cells responsiveness to antidromic and/or synaptic volleys during a sleep-waking cycle. Next, the spontaneous firing of the neurons was recorded during the following sleep-waking cycle. To ensure that fluctuations in responsiveness could occur without concern of ceiling effects, the stimulus intensity was adjusted to straddle threshold (50% responsiveness) in S sleep, when testing usually began. Stimulation was delivered at a rate of 0.2 to 0.5/sec. Unit discharges and focal thalamic slow waves were recorded simultaneously by the microelectrode on direct (50- to 10,000-Hz) and FM (1- to 700-Hz) channels, respectively, of a tape recorder along with trigger pulses and electrographic variables indicating the vigilance state of the animal.

At the end of the experiment, the animals were anesthetized deeply with sodium pentobarbital and perfused with 0.5 liter of saline and 1 liter of 4% formaldehyde by means of an aortic cannula. The positions of the stimulating and recording electrodes and the extent of the pontine lesions were verified in frontal or sagittal frozen sections (50 μm) stained with thionine (Fig. 1). The location of recorded neurons was indicated on photographs of the histological section by combining microlesion sites with micrometer readings.

Analyses. The first statistical analysis concerned the rate and pattern of spontaneous discharge during W, S, and D as defined by electrographic and behavioral criteria (Steriade and Hobson, 1976). Gross movements during W may introduce uncontrolled factors in the evaluation of discharge due to the proprioceptive feedback generated by the movement itself. We therefore analyzed only periods of motionless W, with continuous EEG desynchronization but without phasic bursts of increased EMG activity and eye movements. Similarly, periods (>2 sec) of continuous eye saccades in D sleep were excluded from consideration. The state of S sleep was considered as such only after the transitional period of drowsiness, when the EEG synchronization was no

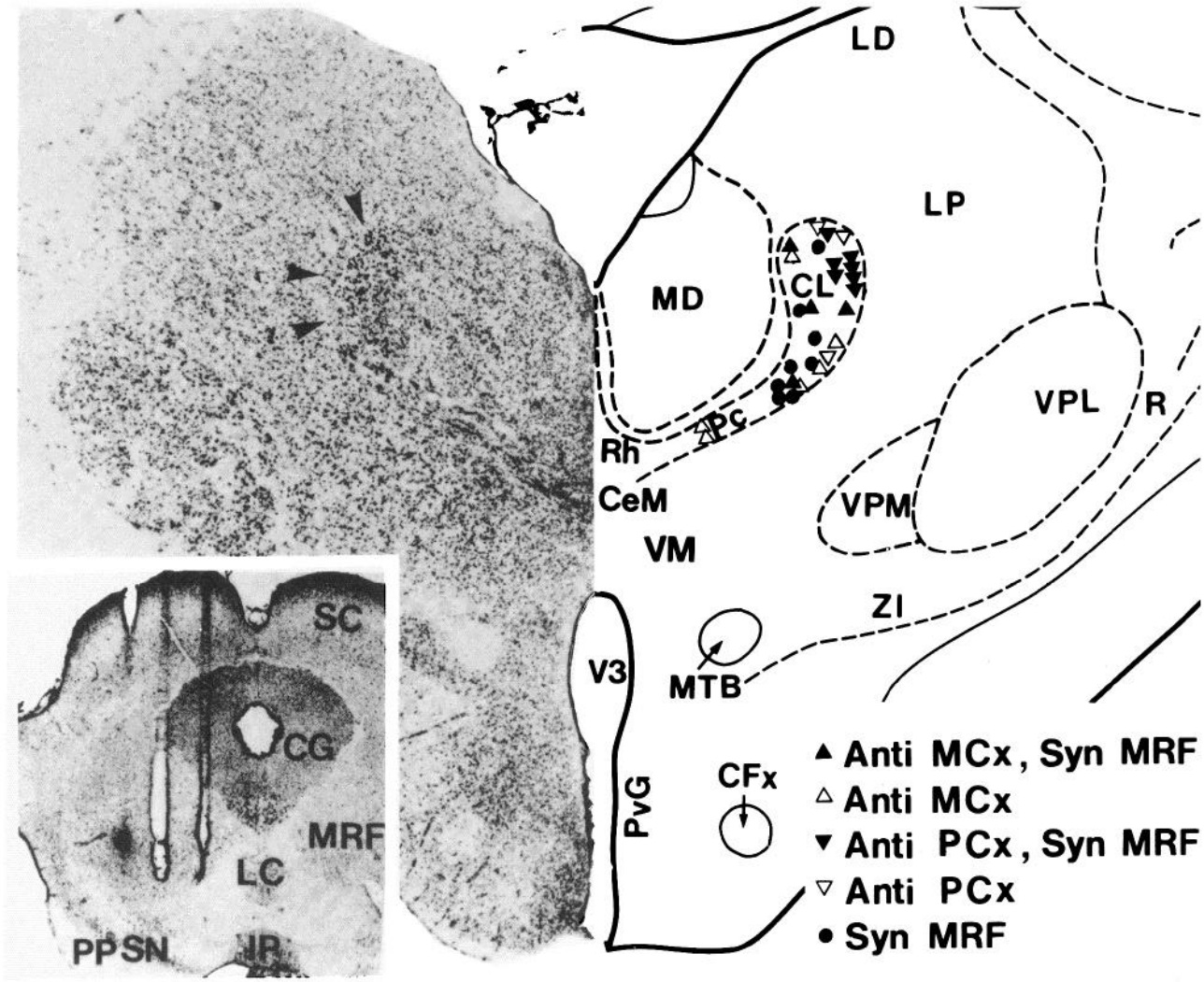

Figure 1. Location of recorded neurons within CL-Pc thalamic nuclei and stimulating electrodes within the MRF (another, lateral MRF electrode was found more anteriorly). The symbols of 28 CL-Pc neurons found between anterior planes 9 and 10 (ipsilateral to the MRF electrodes) and analyzed statistically are drawn at the *right*. See the microelectrode tracks in Steriade and Glenn (1982). Note the group of 7 neurons projecting to the parietal cortex and activated synaptically from the MRF found in the lateral and dorsal parts of the CL (the region of large, deeply staining neurons indicated by the *arrowheads* at the *left*); these fast conducting, high frequency discharging cells are depicted in Figures 2*C*, 5, and 9 (see text). The abbreviations used are: *Anti* and *Syn*, antidromic and synaptic responses; *CeM*, nucleus centralis medialis; *CFx*, columna fornicis; *CG*, central gray; *CL*, nucleus centralis lateralis: *IP*, nucleus interpeduncularis; *LC*, nucleus linearis centralis; *LD*, nucleus lateralis dorsalis; *LP*, nucleus lateralis posterior; *MCx* and *PCx*, motor and parietal cortices; *MD*, nucleus medialis dorsalis; *MTB*, mamillothalamic bundle; *Pc*, nucleus paracentralis; *PP*, pes pedunculi; *PvG*, periventricular gray; *R*, nucleus reticularis; *Rh*, nucleus rhomboidalis; *SC*, superior colliculus; *SN*, substantia nigra; *V3*, third ventricle; *VM*, nucleus ventralis medialis; *VPL* and *VPM*, nuclei ventralis posterolateralis and posteromedialis; *ZI*, zona incerta.

longer interrupted by transient periods of desynchronization. The onset of D sleep was defined as the time of complete muscular atonia. Each epoch included in the analysis was at least 10 sec long and consisted of uninterrupted activity typical of W, S, or D states without phasic motor events. The appropriate epochs of data together with pertinent identification information were transferred and stored in the central campus computer (IBM 3031) operating in an interactive APL/SVA environment. To evaluate the discharge rate and patterns during wake-sleep states, interspike interval histograms were calculated with bins of 0.5 to 20 msec. Antidromic and synaptic responsiveness was assessed from either poststimulus histograms or from multiple sweep arrays (as in Fig. 7*C*).

Results

Data base and neuronal identification

Spontaneous firing and antidromic or synaptic responsiveness were analyzed in 89 CL or Pc neurons during wake-sleep states. Sixty-five of these were backfired by stimulating pericruciate cortical areas 4 or 6 (hereafter referred to as the motor cortex) or anterior suprasylvian cortical areas 5a and 5b (hereafter referred to as the parietal cortex). Forty-seven neurons were activated syn-

aptically from the MRF at latencies under 10 msec. The commonest latencies were 1 to 5 msec. Twenty-three of these neurons also could be identified by antidromic invasion from either the motor or parietal cortex and therefore are included in the former population.

The criteria for antidromic invasion were a fixed latency, collision with either a spontaneously occurring action potential (Fig. 2C_3) or MRF-evoked synaptic discharge (Fig. 2, A_4 and B_3), and the ability to follow fast (>250/sec) stimulation rates. The median conduction velocity of cortically projecting neurons investigated in this study (11.8 m/sec to the motor cortex and 7.8 m/sec to the parietal cortex) is close to that reported for a larger population in a study on the input-output organization of intralaminar nuclei (Steriade and Glenn, 1982). Synaptic excitation from the MRF was differentiated from antidromic invasion by the presence of latency variations over 0.5 msec and a lack of collision with spontaneous discharges at the proper interval.

For the analysis of discharge rates and pattern, statistical descriptions or tests were applied only to those neurons having more than 400 interspike intervals. For the analysis of antidromic and synaptic excitability, at least 20 consecutive trials were required across the different states. By these criteria, 30 neurons were included in the population for discharge pattern analysis and 35 neurons were in the population for excitability analysis. Of the latter, 22 neurons were followed across repeated wake-sleep cycles so that discharge patterns could be studied in the absence of any electrical stimuli.

Spontaneous discharge

All CL-Pc neurons discharged spontaneously in all vigilance states. Two neuronal groups could be distinguished by the following general features.

(*1*) The most numerous group consisted of 82 cells that discharged singly to synaptic activation by MRF stimulation and/or were activated antidromically from the motor or parietal cortex (see Fig. 2, *A* and *B*). These neurons were found throughout the CL-Pc territory and

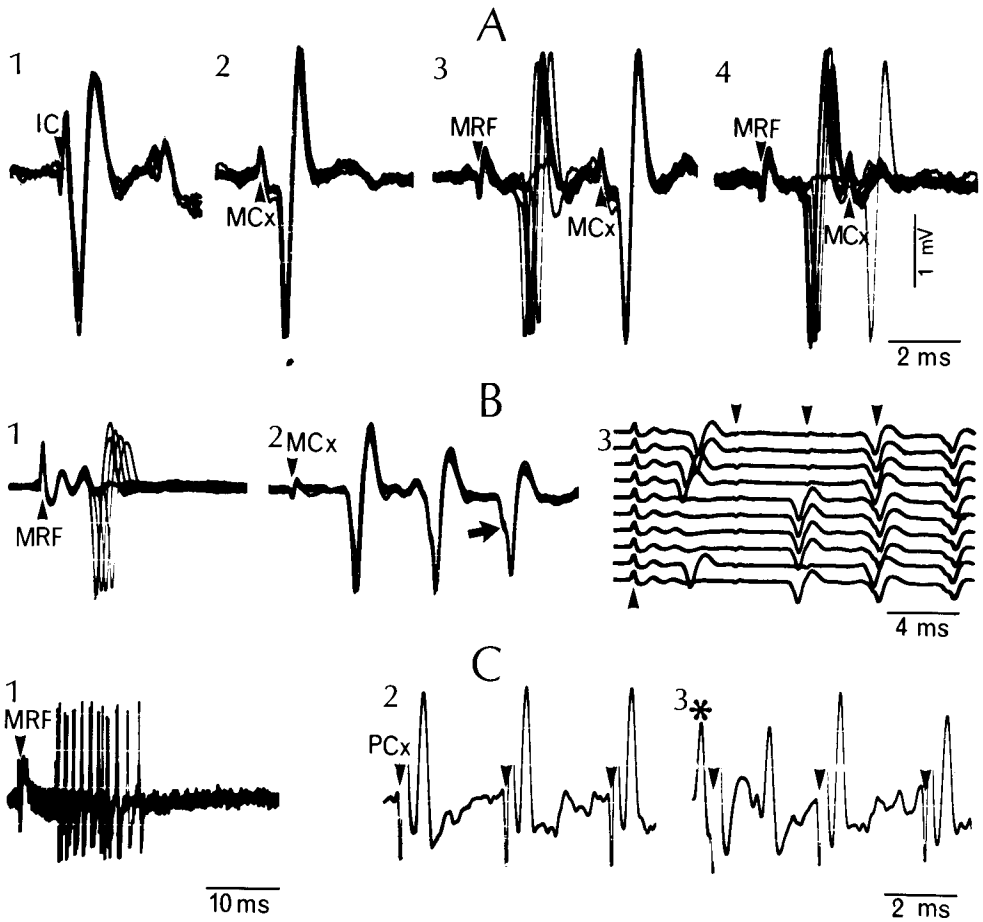

Figure 2. Physiological identification of CL-Pc neurons. Three different cells (*A* to *C*) antidromically activated from the internal capsule (*IC*), motor cortex *MCx*), or parietal cortex (*PCx*) and synaptically driven from the midbrain reticular formation (*MRF*) are shown. Stimulus artifacts are indicated by the *arrowheads* (in B_2, only the first stimulus of a three-shock train at 250/sec is marked). The *arrow* in B_2 indicates fractionation of an antidromically elicited discharge to the last stimulus in the train. A collision between cortically elicited antidromic spikes and a spontaneous discharge (*asterisk* in C_3) or an MRF-evoked synaptic discharge (A_4 and B_3) also appears. Superimposition of 5 to 7 traces (except for C_2 and $_3$) and a 10-sweep sequence with reduced spike amplitude are shown in B_3. In this and following figures, positivity is downard.

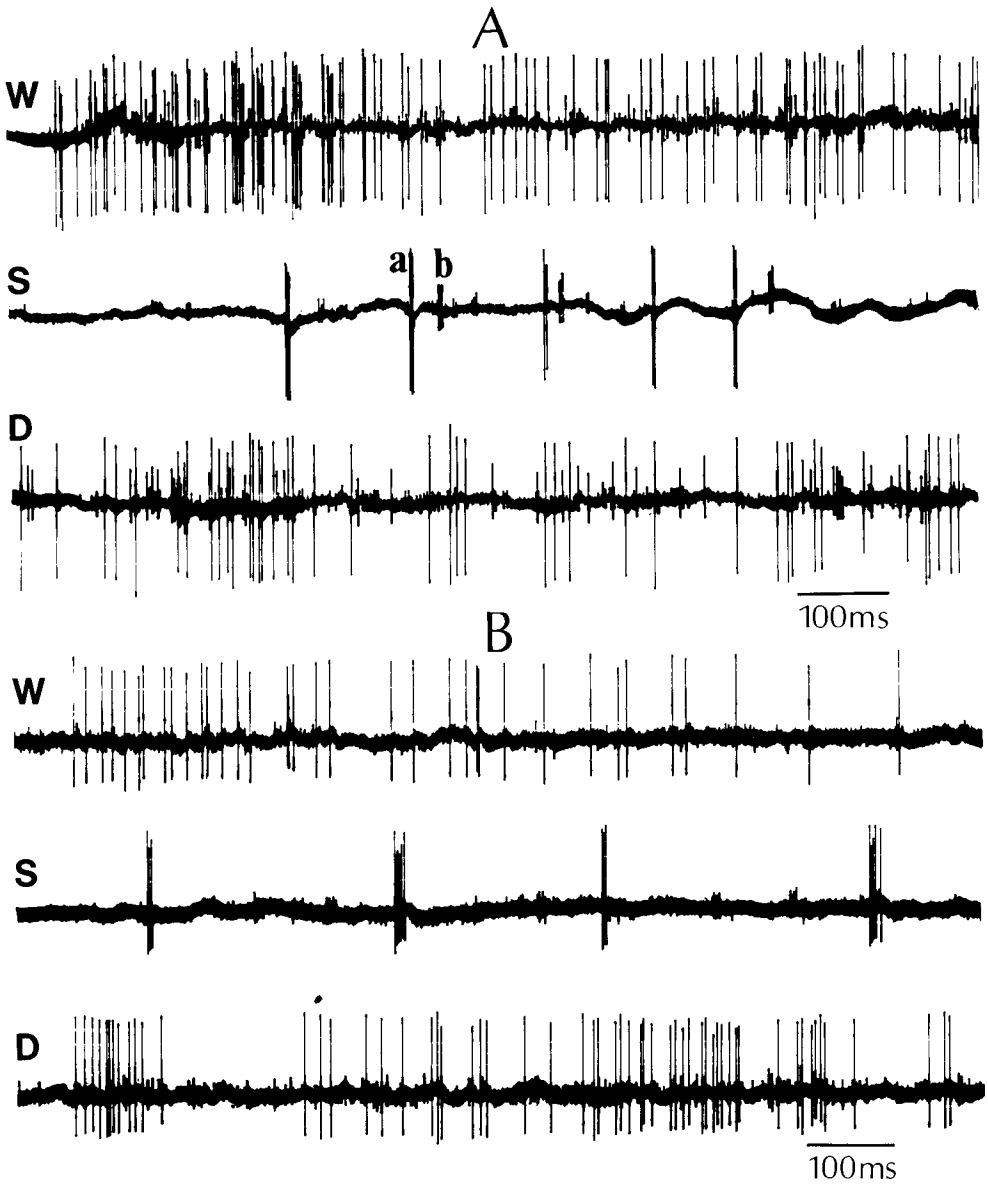

Figure 3. Discharge patterns of cortically projecting CL-Pc neurons during waking (W), synchronized sleep (S), and desynchronized sleep (D). Three neurons (*big* and *small spikes* *a* and *b* in *A* and the *spike* in *B* with 1.3-, 2.2-, and 1.8-msec antidromic response latencies) projected to the motor cortex; *neuron B* also was driven synaptically from the MRF. Note the high frequency spike clusters in S and their replacement by a sustained discharge in W and D.

had no apparent topographical relation to the projection site. Their firing rates and patterns in S sleep were strikingly different from those in desynchronized states (W and D) such that even the audio monitor alone would reveal whether the animal was in S sleep or if it awakened or passed from S to D sleep. During S sleep, cells of this group discharged in short (5- to 10-msec) bursts generally consisting of 3 to 6 spikes at 300 to 600 Hz interspersed with long periods of silence (Fig. 3). During W and D sleep, their firing rate rose. Moreover, the discharge was sustained, lacking the structured bursts that characterized S sleep (Fig. 3). The replacement of the burst-silence pattern by single spikes with a sustained discharge was found during spontaneous shifts from S to full W or D (Fig. 4). The same change occurred transiently with slight sensory stimuli (such as folding the EEG paper) which induced brief EEG desynchronization during S but did not produce overt behavioral signs of arousal.

During S, spike bursts were spaced regularly in 49 of those 82 neurons. Each sequence of bursts consisted of a series of 3- to 5-spike clusters separated by neuronal silence lasting ≃100 to 150 (12 cells) or ≃200 to 350 msec (37 cells), thus resulting in interburst frequencies of 7 to 10 (Fig. 3*A*) and 3 to 5 Hz (Figs. 3*B* and 4*B*). Between burst sequences, some neurons were not completely silent; they could discharge singly or in single bursts (Fig. 4). Burst sequences were closely related in time to both thalamic spindles, recorded as focal slow waves through the same microelectrode, and cortical pericruciate or anterior suprasylvian EEG spindles (Fig. 4*B*). The fre-

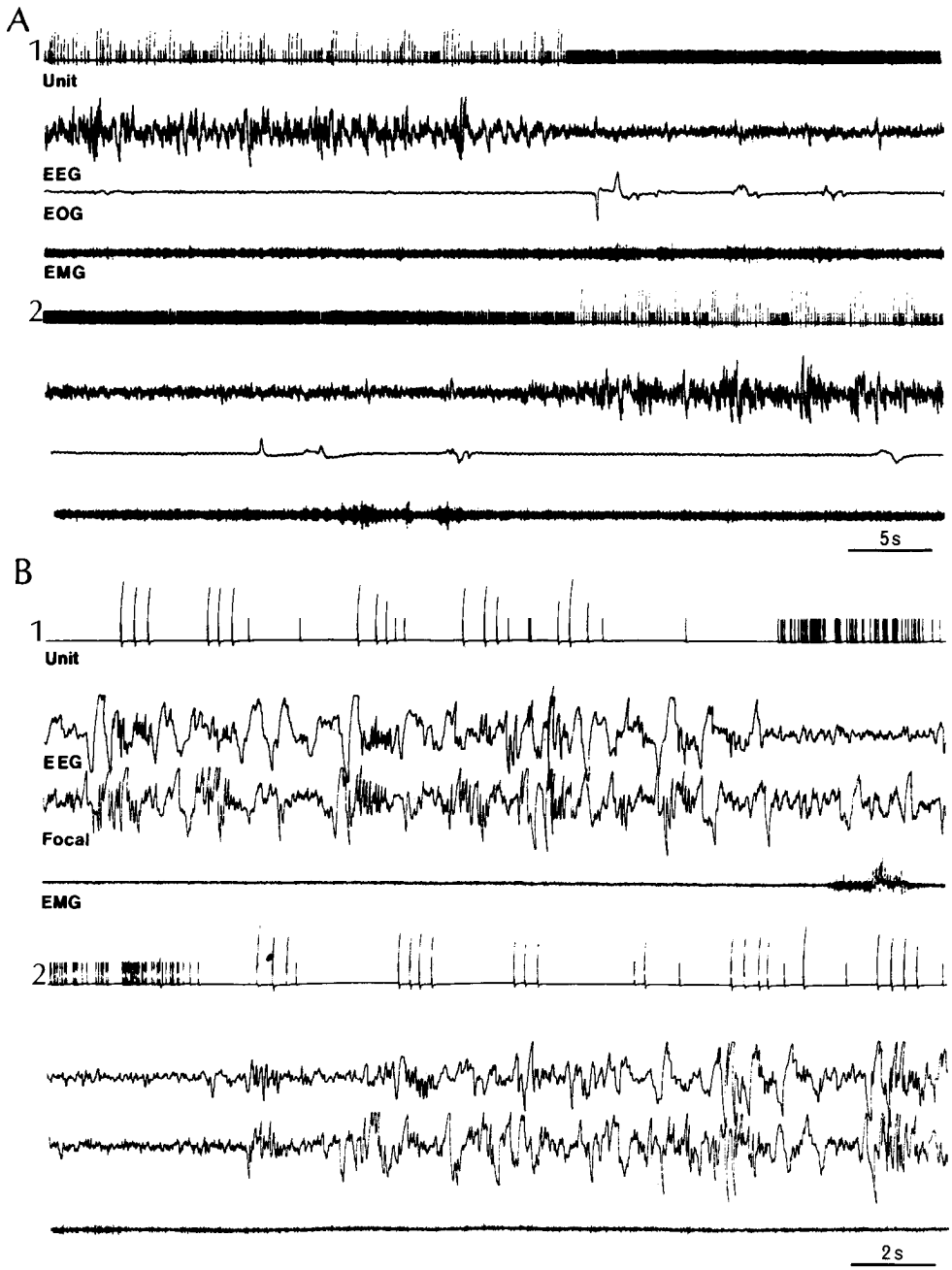

Figure 4. Discharge patterns during transitions from S to W and W to S. Two neurons projecting to the parietal (*A*) and motor (*B*) cortices are shown, *neuron B* is the same as depicted in Figure 3*B*. Unit spikes displayed on the oscilloscope were used to trigger an ink pen galvanometer. The larger deflections represent a burst of high frequency spikes. Note the strikingly different discharge patterns which correlate to EEG activity and other electrographic signs of the behavioral state. In A_2, a decrease in firing rate is seen ≃8 sec prior to the appearance of clustered firing during S. Also note (in B_1 and $_2$) the correlation between sequences of spike bursts and grouped spindle waves as recorded from the cortical surface (*EEG*) and the thalamic microelectrode (*focal*). *EOG*, Electro-oculogram.

quency of EEG spindle waves was 7 to 12 Hz and a majority of neurons exhibited spike bursts at 3 to 5 Hz; nevertheless, the relation between the two kinds of events was evident when 2 or more neurons were recorded simultaneously: the spike bursts of one cell or the other were superimposed on the slow negative components of focal spindle waves.

Interspike interval histograms were computed for 26 cells of this first group, 14 of which were identified antidromically from the motor or parietal cortex (5 also were driven synaptically from the MRF) and 12 of which were excited synaptically at short latencies from the MRF without backfiring from the cortex. Table I shows the summary statistics for rates, modes, and percentage of intervals within various classes in the 14-cell and 12-cell samples (groups A and B, respectively). Appendix 1

TABLE 1

Summary statistics of spontaneous firing (rates, modes, and interval distribution) during wake-sleep states

See the details on the input-output characteristics of neurons belonging to groups A and B and group C in Appendix 1 and the text.

	Rate	Mode	Percentage of Intervals in Different Millisecond Classes			
			<5	5–100	100–500	>500
	impulses/sec	*msec*				
			Waking State			
Groups A and B						
Median	7.86	17.50	1.69	59.55	24.90	5.71
Mean	8.65	25.56	3.31	56.15	28.45	12.09
C.V.[a]	0.52	0.95	1.28	0.36	0.42	1.35
Group C						
Median	51.78	1.25	47.84	48.76	2.55	0.06
Mean	49.50	1.35	48.61	48.43	2.85	0.11
C.V.	0.40	0.20	0.66	0.67	0.89	1.30
			Synchronized Sleep			
Groups A and B						
Median	3.66	2.25	28.55	25.84	22.67	16.28
Mean	3.78	5.13	32.61	28.11	23.02	16.27
C.V.	0.44	2.33	0.56	0.76	0.32	0.56
Group C						
Median	32.30	1.05	74.44	13.15	8.85	2.38
Mean	28.40	1.08	73.16	14.92	8.98	2.95
C.V.	0.54	0.12	0.18	0.79	0.22	0.85
			Desynchronized Sleep			
Groups A and B						
Median	8.40	10.00	7.06	58.49	20.19	5.20
Mean	11.05	15.77	10.32	57.24	21.98	10.46
C.V.	0.69	1.12	0.91	0.22	0.47	1.13
Group C						
Median	30.02	1.25	56.07	38.51	9.10	0.32
Mean	30.40	1.35	51.07	38.37	9.99	0.56
C.V.	0.25	0.27	0.30	0.48	0.45	1.27

Groups A and B	Statistical Significance (Mann-Whitney Test)		
	Rate	Mode	<5-msec Intervals
W-S (26-26 cells)	0.0005	0.0005	0.0005
S-D (26-11 cells)	0.002	0.001	0.001
W-D (26-11 cells)	0.75	0.15	0.02

[a] C.V., coefficient of variation.

provides further details on each of these 26 cells. The Mann-Whitney U test shows no significant differences between the two (14-cell and 12-cell) groups with regard to rates, modes, and percentage of intervals under 5 msec in W ($p < 0.75$ to 1) and S ($p < 0.08$ to 0.75). We therefore assumed that neurons of the two samples could be treated together and applied the Mann-Whitney test to compare first order measures across states for all 26 neurons during W and S and for 11 of them during D.

The salient findings follow. (*a*) Firing rates doubled from S to either W or D. The rate difference between S and either W or D is highly significant ($p < 0.0005$ and 0.002, respectively), while it is not significant between W and D ($p < 0.75$). (*b*) During S, most interval durations were found in the <5-msec class, with modes of 2.5 msec, reflecting the intraburst frequencies. During W and D states, the majority of intervals were found between 5 and 100 msec, usually with modes longer than 10 msec. The modes as well as the percentage of intervals <5 msec were significantly different in S from both W and D ($p < 0.005$ and 0.001, respectively). The modes did not differ in D from W ($p < 0.15$), but more intervals <5 msec were found in D than in W ($p < 0.02$). (*c*) A late, minor mode was detected in S for 16 out of 26 neurons. This late mode usually ranged between 200 and 350 msec (Appendix 1), reflecting the interburst silent periods. An interval of this density did not appear in W and D in spite of the fact that the percentage of intervals in the 100- to 500-msec class were not different from those in S.

(*2*) A second group of 7 CL neurons were treated separately because of their homogeneity. All cells were driven synaptically from the MRF in bursts of unusually

high frequency (800 to 1,000 Hz) and they all projected to the parietal cortex with very high conduction velocities (30 to 50 m/sec), in fact, 4 times faster than other CL neurons projecting to area 5 (see Fig. 2*C*). To add to these features, all of these cells were localized histologically in the laterodorsal part of CL where large, deeply staining cells are found (see Steriade and Glenn, 1982). The differences in the discharge characteristics of this neuronal group as compared to those of the former group follow. (*a*) The discharge rate exceeded 30 Hz in each state (4 times higher than in the first group). The discharge rate was generally highest in W. (*b*) During S, these neurons fired in bursts of 8 to 10 spikes at 800 to 1,000 Hz; when bursts were grouped, their frequency was 8 to 10 Hz (Fig. 5). During W and D, the bursts did not disappear as they did for the first group. Instead, the intraburst frequency remained as high as in S, but the burst *duration* was reduced considerably (from 8 to 10 to 2 to 5 spikes). Series of bursts could reach frequencies of 20 to 40 Hz (Fig. 5).

The interspike interval histograms in 4 of the above neurons (group C in Table I and Appendix 1) show high discharge rates and an excessively short mode (around 1.0 to 1.25 msec), reflecting the intraburst frequency of 800 to 1,000 Hz. Statistical tests for state effects cannot be made in such a limited sample, yet we note that the modes were shorter in S than W or D, the percentage of intervals in the <5-msec class was higher in S, and the percentage of medium intervals (5 to 100 msec) was higher in W and D for all neurons.

The unusually high intraburst frequencies of the discharges of these neurons were not due to mechanical infringements by the microelectrode. Indeed, injured cells cannot sustain repetitive firing for periods longer than 10 to 15 min, whereas these neurons were recorded during multiple sleep-waking cycles without any significant change in spike amplitude (Fig. 5). The spikes moreover were initially negative, indicating that the microelectrode was at least some distance from the cell, and the spikes did not have notches on the rising phase, fractionations, or abnormal durations or time courses (see one of these cells also in Fig. 9).

Cell responsiveness

Antidromically elicited discharges. Out of 65 neurons with identified neocortical projections, 19 were recorded for sufficient time during well defined behavioral states to permit quantitative measurements of fluctuations in antidromic responsiveness at juxtathreshold intensity (see "Materials and Methods"). All 19 neurons analyzed quantitatively for antidromic activation from the motor or parietal cortex had enhanced responsiveness in both W and D states as compared to S sleep. The antidromic responsiveness of the whole sample (Fig. 6) increased by ≃60% in desynchronized states (W and D). There was, of course, a significant difference between W and S ($p < 0.0005$; see details on individual neurons in Appendix 2). A selected example of this increased responsiveness in W and D states is shown in Figure 7*C*. In some cases, the enhanced probability of discharge during W could be seen in conjunction with a reduction in the delay between the initial segment (IS) and soma-dendritic (SD) spike observed during S (Fig. 7*B*) or in conjunction with a transformation from IS spikes in S to SD spikes in W (Fig. 7*A*). In 6 out of 19 neurons, increased antidromic responsiveness to levels seen in fully developed W and D states was found 10 to 25 sec in advance of EEG desynchronization at both S-to-W and S-to-D transitions (Fig. 7*D*). As a rule, the diminished antidromic responsiveness

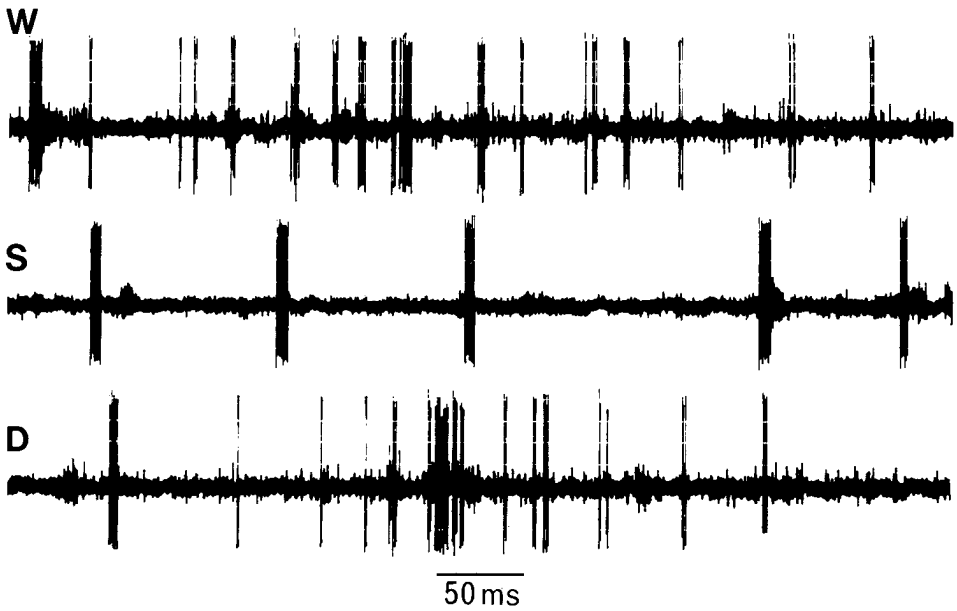

Figure 5. Discharge patterns of a fast conducting (50 m/sec) CL neuron projecting to area 5 (antidromic response latency, 0.3 msec) and synaptically driven from the MRF with a spike barrage at a frequency of 800 to 1,000 Hz (same neuron as depicted in Fig. 9). Spontaneous bursts in S consisted of 8 to 10 discharges at 800 to 1,000 Hz. Note the persistence of spike bursts during W and D but with a decreased duration and shorter interburst periods.

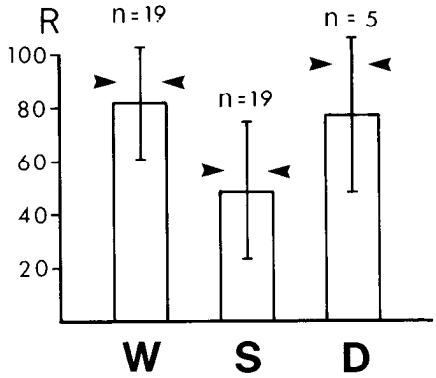

Figure 6. The median (*arrowheads*), mean (*columns*), and standard deviation (*bars*) for the percentage of antidromic responses in a sample of 19 CL-Pc neurons during W and S. Five of these neurons were recorded during D (see the details on each cell in Appendix 2). *R*, Percentage of stimuli that evoked an antidromic action potential.

from W to S took place on a background of decreased averaged discharge rates (Fig. 7*A*; see also the values of both spontaneous firing and antidromic responsiveness in 12 cells in Appendixes 1 and 2). Lastly, the decreased antidromic responsiveness seen in S was associated with an increased occurrence of postinhibitory rebounds (Fig. 7*A*). The details of the rebound are to be reported fully elsewhere (see also Steriade et al., 1977).

Synaptically evoked discharges. Synaptic responses to MRF stimulation at latencies shorter than 5 msec were analyzed in 16 CL-Pc neurons during wake and sleep states. Of them, 12 cells discharged singly or with 2 spikes at distinct latencies, and 4 fired bursts at 800 to 1,000 Hz (groups A B and group C, respectively, in Appendix 1). Conclusions on changes in cell excitability to orthodromic volleys are difficult to assess in extracellular recordings unless the responses indicate monosynaptic activation and clear-cut alterations are observed across behavioral states. Nine neurons which were driven monosynaptically from the MRF did change their excitability spectacularly during different states. The criterion of monosynaptic activation was the shortest latency—<1.5 msec—that the cell reached in either state of the sleep-waking cycle. This value is the sum of the utilization and discharge initiation time (≃0.3 msec), minimum conduction time (0.8 msec) as determined from studies on MRF neurons antidromically activated from intralaminar thalamic nuclei (Ropert and Steriade, 1981), and the synaptic delay (≃0.4 msec). In these 9 neurons, signs of increased synaptic excitability were seen in W and D states compared to S sleep. These signs were of three types, which are illustrated by the 3 neurons depicted in Figures 8 and 9. (*a*) The probability of single spike responses increased from 20 to 40% in S to 70 to 90% in either W or D (Fig. 8*A*). (*b*) For synaptic responses consisting of two discharge groups, a dramatic decrease in responsiveness affected the early group (1 to 2 msec bin) during S, which contrasted with intact secondary excitation at 12 to 20 msec (Fig. 8*B*). (*c*) In the peculiar group of fast conducting CL neurons which discharged repetitively at 800 to 1,000 Hz to MRF volleys, the latency to the initial discharge in the burst varied in different cells from 2.5 to 5 msec during S, but it reduced to 1.0 to 2.0 msec during either W or D. At the same time, the duration of the high frequency barrage diminished from 5 to 7 spikes in S to 2 to 3 spikes in W or D (Fig. 9). This phenomenon seen for MRF-evoked synaptic responses is similar to the reduction in duration of spontaneously occurring bursts during EEG-desynchronized states (see above, Fig. 5).

Discussion

Tonic activation of the cerebral cortex during EEG-desynchronized states. This study has revealed that W and D are similar with regard to the discharge patterns and excitability of cortically projecting intralaminar thalamic neurons that relay MRF activity. In both EEG-desynchronized states, the rates of spontaneous firing are increased, first order statistics show a tonic pattern with a great predominance of medium (5- to 100-msec) intervals, soma responsiveness to antidromic stimulation is enhanced, the probability of synaptically elicited single discharges is increased, and the latency and duration of high frequency bursts evoked by synaptic volleys are shortened. All of these events fit in well with the definition of thalamocortical activation processes at a cellular level (Steriade, 1981). Three features of the present study bear enumeration. (*a*) Firstly, the conclusion on W-D similarity was drawn from a battery of tests that analyzed the spontaneous discharge in conjunction with antidromic and synaptic responsiveness. A concerted investigation of spontaneous and evoked activities is essential because certain classes of cortical and thalamic neurons are known to diminish their discharge rate or even to cease firing altogether, while the antidromically or synaptically evoked firing is enhanced simultaneously (Steriade et al., 1974; Livingstone and Hubel, 1981). The parallel changes in spontaneous and evoked firing observed in intralaminar neurons lead to a simple, convergent explanation of the results: intralaminar thalamic neurons are facilitated tonically during W and D. (*b*) Secondly, we herein explored the particular thalamic nuclei that are the best candidates underlying influences over widespread neocortical regions. Sensory, motor, and associative nuclei project predominantly toward the middle layers of their respective cortical area. From among the other class of nuclei, the so-called nonspecific nuclei because of their projectons to more than one cortical region and their afferentation from heterogeneous sources, a number can be conditionally ruled out. The centrum medianum-parafascicularis complex projects densely to the striatum (Jones and Leavitt, 1974) but has few corticopetal axons, and these may project only to a localized field of the frontal pole (Condé and Condé, 1979; Herkenham, 1980; Jones, 1981). The projection of the ventralis medialis nucleus is widespread and terminates in layer I of the cortex but is restricted in the cat to motor and premotor precruciate areas (Glenn et al., 1982). The efferents of the intralaminar CL-Pc nuclei, on the other hand, distribute to precruciate, postcruciate, and anterior suprasylvian gyri (Jones and Leavitt, 1974; Itoh and Mizuno, 1977; Hendry et al., 1979; Steriade and Glenn, 1982) and, to a lesser extent, to the SII, auditory cortex, posterior suprasylvian gyrus (Macchi et al., 1977), and extrastriate cortex (Kennedy and Baleydier, 1977).

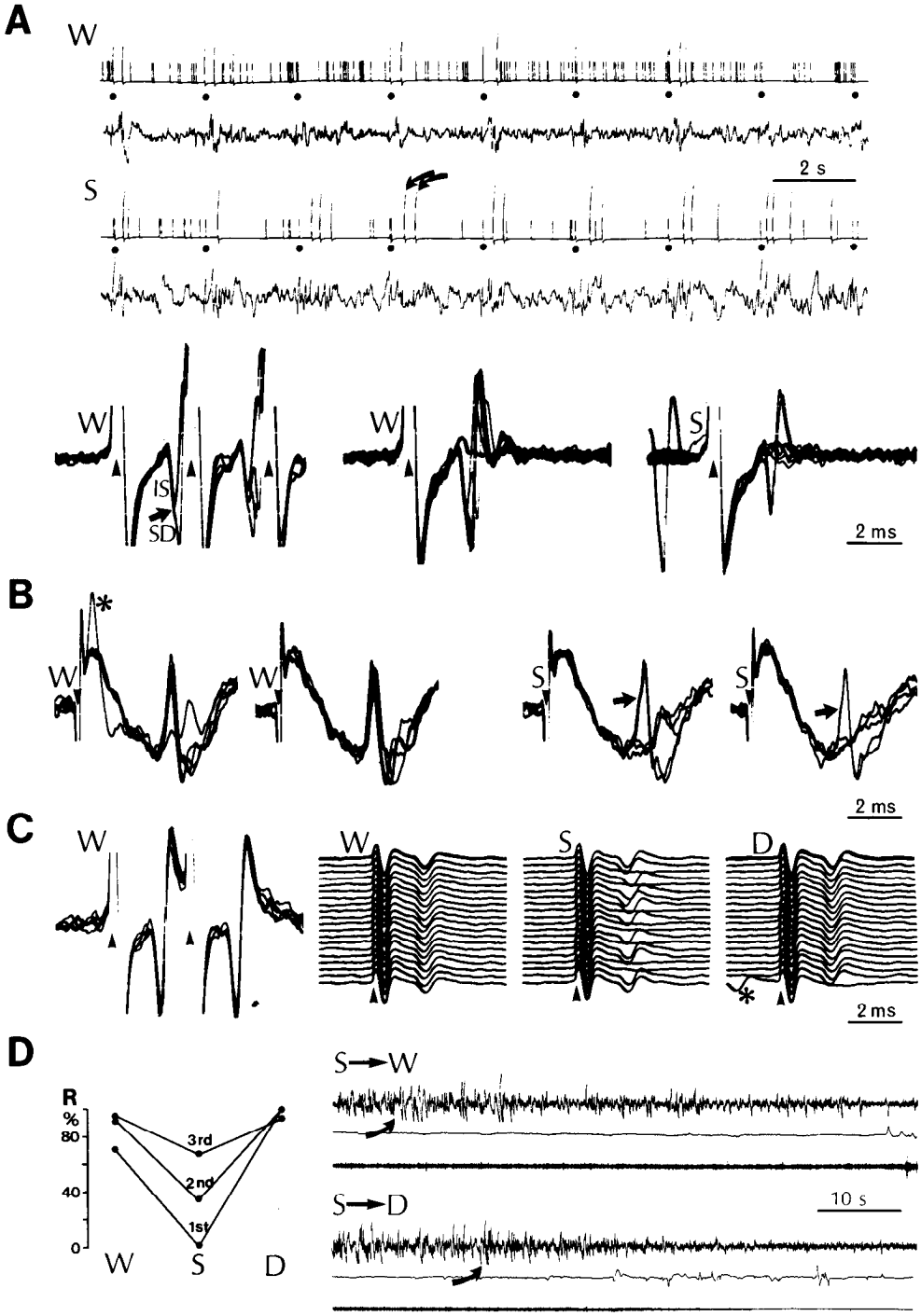

Figure 7. Antidromically elicited discharges during W, S, and D states. Four different neurons activated from the motor (*B*) and parietal (*A*, *C*, and *D*) cortices were recorded. Stimulus artifacts are marked by *arrowheads*. *A* (cell 51-2-7 in Appendix 2), The top ink pen record depicts the spontaneous and evoked unit activities (*first trace*) and EEG (*second trace*). The records are separated by ≃30 sec. Shown are: (*a*) the decreased rate of spontaneous firing in S; (*b*) the absence of full antidromic spikes in S (*dots* indicate applications of single shocks; when the deflection above the *dots* is small, it reflects stimulus artifact, whereas when large, a full antidromic spike is indicated; from nine stimuli, six full antidromic responses are evoked in W and none in S); (*c*) the more common occurrence of single or double postinhibitory spike bursts (rebounds) in S (*two oblique arrows*). Below are antidromic discharges during W and S. Note the notched and full spikes in W in contrast to only IS spikes in S (during S, a full spontaneous spike is shown in one sweep, , before the stimulus artifact, for comparison). *B*, Diminished antidromic responsiveness and increased IS-SD delay (*arrows*) in S as compared to W; a spontaneous discharge (*asterisk*) in W collides with an antidromic spike. *C* (cell 18-3-2 in Appendix 2), Diminished antidromic responsiveness in S as compared to either W and D. The *asterisk* shows a collision with a spontaneous discharge. *D* (cell 17-2-8 in Appendix 2, same as depicted in Fig. 2*C*), The percentage of antidromic responses after the first, second, and third stimuli in a 350-Hz train (as in Fig. 2*C*) in W, S, and D. The times at which responsiveness to the first shock was first detected to increase in S-to-W and S-to-D transitions are indicated by *oblique arrows*. *R*, Percentage of stimuli that evoked an antidromic action potential.

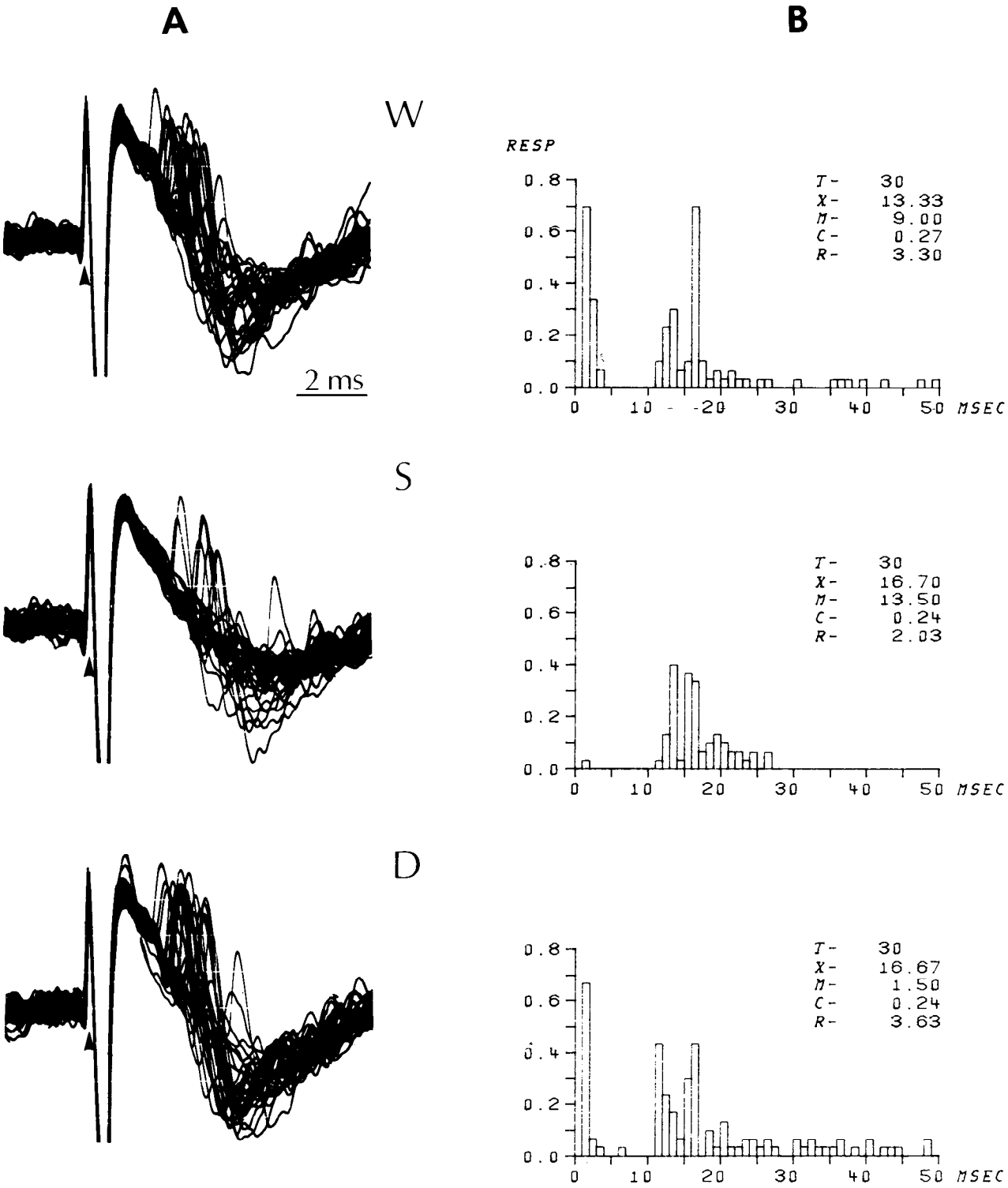

Figure 8. Synaptically elicited discharges during W, S, and D. Two neurons were activated from MRF (*A* and *B*). *A*, Thirty superimposed sweeps in each state. Stimulus artifacts are marked by *arrowheads*. *B*, Poststimulus histograms with 1-msec bins. Note the virtual disappearance of early discharges (1 to 2 msec) during S in contrast to the preservation of discharges evoked at longer latencies (12 to 20 msec). The abbreviations used are: *Resp*, number of spikes per bin divided by number of trials; *T*, number of trials; *X*, mean latency; *M*, latency mode; *C*, coefficient of variation; *R*, sum of all *Resp.* on the depicted ordinate. In *B*, during W, the indicated mode of 9.0 msec denotes the average of two equal amplitude modes at 1.5 and 16.5 msec.

In contrast with the projections from some thalamic nuclei to a restricted cortical region, the axons of CL-Pc origin arborize in layer I and possibly layer VI (Jones and Leavitt, 1974; Foster, 1980; Herkenham, 1980) of areas belonging to multiple sensory and motor systems. (*c*) Lastly, the neurons analyzed physiologically in this study were found to project to the neocortex and to receive monosynaptic excitation from the MRF. These neurons

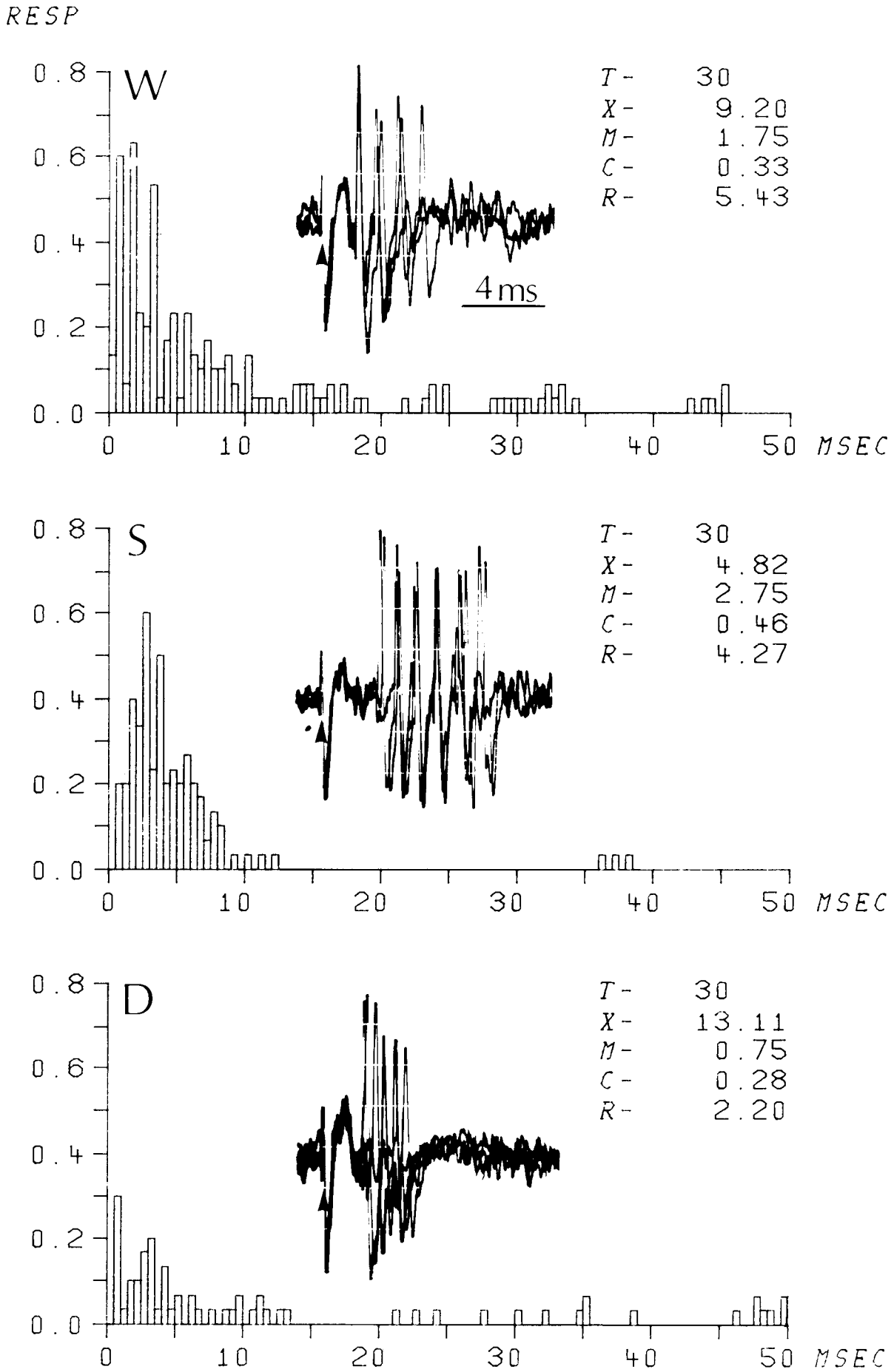
RESP
W
T- 30
X- 9.20
M- 1.75
C- 0.33
R- 5.43
4ms
0.8
0.6
0.4
0.2
0.0
0
10
20
30
40
50
MSEC
S
T- 30
X- 4.82
M- 2.75
C- 0.46
R- 4.27
D
T- 30
X- 13.11
M- 0.75
C- 0.28
R- 2.20

therefore constitute a relatively homogeneous population in CL-Pc intralaminar nuclei that are involved in the transfer of ascending reticular influences. The midbrain reticular neurons with axons distributing to intralaminar thalamic nuclei are located within the nucleus cuneiformis and its ventrorostral extension, the central tegmental field, as shown by autoradiography (Edwards and De Olmos, 1976) and antidromic identification experiments (Ropert and Steriade, 1981).

The similarity in the increased excitability of cortically projecting intralaminar thalamic neurons during both desynchronized states (W and D) suggests that the CL-Pc nuclei, along with the MRF, are endowed with tonic activating properties. The reticular activating concept was based on experiments using electrical stimulation and lesion (see Moruzzi's (1972) review) that may have affected passing fibers arising in other brainstem structures. This difficulty in interpretation and the discovery of extensively projecting monoaminergic systems led to a challenge of the reticular concept and to hypotheses on the role of noradrenergic fibers issuing from the anterior part of the locus coeruleus in tonic activation of the forebrain, particularly during arousal and waking (Jouvet, 1972). It is worthwhile to specify the reasons why the midbrain reticular core and its major rostral target, the intralaminar thalamus, rather than the locus coeruleus, probably mediate tonic cortical activation in the EEG-desynchronized states. (*a*) MRF stimulation elicits an enhanced excitability of thalamic and cortical long axon cells as expressed by increased rates of spontaneous discharge associated with increased responsiveness to antidromic or monosynaptic stimulation (reviewed in Steriade and Hobson, 1976). MRF stimulation reduces the duration of inhibitory periods and causes a blockade of cyclic inhibitory-rebound sequences (Purpura, 1970; Steriade et al., 1971, 1977; Singer, 1977). All of these events evoked by MRF stimulation mimic the features found in the natural W state in behaving animals (Steriade, 1981). Contrariwise, stimulation of the locus coeruleus or iontophoretic application of norepinephrine produces hyperpolarization and decreased rates of spontaneous firing in cortical and thalamic long axon cells (Stone et al., 1975; Phillis and Kostopoulos, 1977; Reader et al., 1979; Rivner and Sutin, 1981). These effects are not compatible with the role of tonically potentiating thalamic and cortical processes. Instead, the locus coeruleus could function in phasic processes, increasing the signal-to-noise ratio and biasing behavioral orientation toward relevant events (Foote and Bloom, 1979; Aston-Jones and Bloom, 1981b). (*b*) The same constellation of cortical cellular events induced by MRF stimulation or natural W also is found during D. The available evidence indicates that thalamocortical (present data) and corticofugal neurons (Steriade, 1981) behave similarly during W and D. Cortical activation processes probably are caused by cholinergic facilitation (Krnjević, 1981) and the cortical release of acetylcholine is higher in both W and D states as compared to S (Jasper and Tessier, 1971). In keeping with these findings, statistical measures of discharge rates and patterns in rostrally projecting MRF neurons in D were found to be much closer to W than to S (Steriade et al., 1982). On the contrary, locus coeruleus neurons have a polar behavior during W and D such that discharge is virtually absent in the latter state (Chu and Bloom, 1974; Hobson et al., 1975; Aston-Jones and Bloom, 1981a). The polar state dependence is again incompatible with the role of the locus coeruleus in tonic activation during both W and D. (*c*) Finally, normal desynchronization of the EEG survives the bilateral destruction of the locus coeruleus resulting in a 85% to 95% depletion of cortical norepinephrine (Jones et al., 1977).

The increased excitation of rostrally projecting MRF neurons during activated states (Steriade et al., 1982) is relayed by CL-Pc neurons and transferred toward the neocortex. The influences exerted by cortically projecting neurons of the thalamic intralaminar nuclei are excitatory in nature as indicated by the depolarization, increased rate of neuronal firing and enhanced responsiveness of cortical neurons during stimulation of the medial intralaminar nuclei (Klee et al., 1964). These effects are compatible with the findings of Donoghue and Ebner (1981) in the opossum showing that fibers of intralaminar thalamic origin form round asymmetrical synapses with dendrites in the outer part of layer I. The notion that intralaminar nuclei exert a depolarizing action at the cortical surface is strengthened by the current density pattern of CL-evoked field potentials in the suprasylvian gyrus of cat (Foster, 1980). The cortical effect of intralaminar nuclei is synergic with excitatory events elicited by MRF stimulation, which also start in superficial cortical layers (Inubushi et al., 1978a, b). Moreover, the CL-evoked cortical potentiation of sensory responses may be independent of the rostral reticular core because it can be elicited in high cerveau isolé preparations (Steriade and Demetrescu, 1960). We believe that the depolarization evoked by axons of CL-Pc origin in distal parts of the apical dendrites of cortical neurons is a major factor of activation, defined as a tonic state of readiness in neuronal networks (Steriade, 1981), thus creating the necessary background for potentiation of neuronal responses during attentive behavior (Mountcastle et al., 1981). A laminar analysis showed that attentive behavior most strongly influenced neurons at the junction of layers I and II and in layer VI (Hyvärien et al., 1980), which are the sites of arborization of axons arising in intralaminar nuclei (see above). It is conceivable that, by cutting off the ascending drive of intralaminar thalamic origin, one would create favorable conditions for cortical deactivation and unattentive behavior, thus producing the predisposition to lethargy and sleep (Façon et al., 1958).

The similarity between W and D concerns the EEG desynchronization and the basic processes of rostral re-

Figure 9. MRF-evoked high fequency burst in a fast conducting CL neuron projecting to area 5 during W, S and D (cell 17-2-5 in Appendixes 1 and 2; same neuron as in Fig. 5). Superimposed sweeps and poststimulus histograms with 0.5-msec bins are shown. Note the shorter latency and diminished duration of bursts in W and D. The abbreviations on the poststimulus histograms are defined in the legend to Figure 8.

ticular, thalamic, and cortical neurons. At least, the marked differences in the mental content between these two states could be ascribed to the opposite behavior of monoaminergic (coeruleus and raphe) neurons in W and D. The virtual cessation of discharge in aminergic neurons during D sleep probably results in disinhibition of yet unclear structures in the neo- and allocortex.

Clustered firing during S sleep. Bursting discharge during natural EEG synchronization is a feature that CL-Pc neurons share with cells in other thalamic nuclei specifically projecting to the visual (Hubel, 1960; Sakakura, 1968; Mukhametov et al., 1970), somatosensory (Baker, 1971; Benoit and Chateignier, 1973), parietal association (Steriade et al., 1977; Fourment and Hirsch, 1979), and motor (Lamarre et al., 1971; Steriade et al., 1971) cortices. The thalamic burst can be defined as a brief, stereotyped event consisting of a structured group of high frequency spikes (usually 300 to 400/sec, but see 800 to 1,000/sec in Fig. 5). As such, the spike barrage in cortically projecting neurons of the dorsolateral thalamus can be clearly differentiated from repetitive discharges spread over longer durations, with lower and variable frequencies, which occur during sleep in long axon cortical (Evarts, 1964; Steriade et al., 1974) and cerebellothalamic (Steriade et al., 1971) neurons. The idea that the short, high frequency bursts during S are a thalamically generated phenomenon is supported by the lack of burst patterns in thalamopetal fibers during S (Mukhametov et al., 1970; Lamarre et al., 1971; Benoit and Chateignier, 1973) and unchanged burst patterns in ventrolateral or CL-Pc thalamic neurons following cerebellar nuclear destruction (Steriade et al., 1971) or midbrain transections combined with decortication (manuscript in preparation). Moreover, during the present experiments, we found that, by advancing the microelectrode outside of the thalamic limits into the lateral hypothalamus and subthalamus, neurons dramatically changed their discharge patterns during S, with a virtual lack of intervals <5 msec.

The basic prerequisite for thalamic bursting may be a hyperpolarization of neurons. Recent experiments by Deschênes et al. (1982), using intracellular recordings of ventrolateral thalamic neurons, have revealed that hyperpolarization of the cell membrane by current injections or occurring spontaneously uncovers a conductance which is normally inactive at the resting membrane potential level. The conductance is voltage and time dependent. Once it is uncovered by hyperpolarization, it can be activated by either depolarizing current pulses or synaptic potentials. The response consists of a spike burst like that which is found during S sleep in behaving animals. In fact, the first event in a transition from EEG-desynchronized to EEG-synchronized states is a period of reduced spontaneous discharge or even complete silence of firing in thalamic neurons that precedes the appearance of spike bursts associated with EEG spindling (Fig. 3*B* in Steriade et al., 1971; see also the present Fig. 4). The early diminished firing rate probably is due to a disfacilitation as a consequence of the sudden withdrawal of tonic excitatory impulses of rostral reticular origin at sleep onset (see Fig. 32*C* in Steriade, 1980). That long lasting hyperpolarizing potentials prevail in thalamic neurons during S sleep is shown by the IS-SD break of antidromically elicited discharges or even IS spikes in isolation at this time (see Fig. 8, *A* and *B*). It is known from studies on spinal motoneurons that the IS-SD break can be induced by hyperpolarization either from injected currents (Coombs et al., 1955) or from IPSPs elicited by stimulating descending pathways (Llinas and Terzuolo, 1964). The final effect of long lasting inhibitory potentials in thalamic neurons is a potent blockade of the transmission of impulses traveling in ascending pathways (Steriade et al., 1969), which provides a mechanism for closing channels, a necessary prelude to reach genuine manifestations of sleep.

References

Aston-Jones, G., and F. E. Bloom (1981a) Activity of norepinephrine-containing locus coeruleus neurons in behaving rats anticipates fluctuations in the sleep-waking cycle. J. Neurosci. *1:* 876–886.

Aston-Jones, G., and F. E. Bloom (1981b) Norepinephrine-containing locus coeruleus neurons in behaving rats exhibit pronounced responses to non-noxious environmental stimuli. J. Neurosci. *1:* 887–900.

Baker, M. A. (1971) Spontaneous and evoked activity of neurones in the somatosensory thalamus of the waking cat. J. Physiol. (Lond.) *217:* 359–379.

Benoit, O., and C. Chateignier (1973) Patterns of spontaneous unitary discharge in thalamic ventrobasal complex during wakefulness and sleep. Exp. Brain Res. *17:* 348–363.

Chu, N. S., and F. E. Bloom (1974) Activity patterns of catecholamine-containing pontine neurons in the dorso-lateral tegmentum of unrestrained cats. J. Neurobiol. *5:* 527–544.

Condé, F., and H. Condé (1979) Observations on the orthograde and retrograde transport of horseradish peroxidase in the cat. J. Hirnforsch. *20:* 35–46.

Coombs, J. S., J. C. Eccles, and P. Fatt (1955) The electrical properties of the motoneurone membrane. J. Physiol. (Lond). *130:* 291–325.

Deschênes, M., J. P. Roy, and M. Steriade (1982) Thalamic bursting mechanism: An inward slow current revealed by membrane hyperpolarization. Brain Res. *239:* 289–293.

Donoghue, J. P., and F. F. Ebner (1981) The laminar distribution and ultrastructure of fibers projecting from three thalamic nuclei to the somatic sensory-motor cortex of the opossum. J. Comp. Neurol. *198:* 389–420.

Edwards, S. B., and J. S. De Olmos (1976) Autoradiographic studies of the projections of the midbrain reticular formation: Ascending projections of nucleus cuneiformis. J. Comp. Neurol. *165:* 417–432.

Evarts, E. V. (1964) Temporal patterns of discharge of pyramidal tract neurons during sleep and waking in the monkey. J. Neurophysiol. *27:* 152–171.

Facon, E., M. Steriade, and N. Wertheim (1958) Hypersomnie prolongée engendrée par des lésions bilatérales du système activateur médial. Le syndrome thrombotique de la bifurcation du tronc basilaire. Rev. Neurol. (Paris) *98:* 117–133.

Foote, S. L., and F. E. Bloom (1979) Activity of norepinephrine-containing locus coeruleus neurons in the unanesthetized squirrel monkey. In *Catecholamines: Basic and Clinical Frontiers*, E. Usdin, I. Kopin, and J. Barchas, eds., pp. 625–627, Pergamon Press, Elmsford, NY.

Foster, J. A. (1980) Intracortical origin of recruiting responses in the cat cortex. Electroencephalogr. Clin. Neurophysiol. *48:* 639–653.

Fourment, A., and J. C. Hirsch (1979) Single-unit discharges in the dorsolateral thalamus of behaving cats: Spontaneous activity. Exp. Neurol. *65:* 1–15.

Glenn, L. L., J. Hada, J. P. Roy, M. Deschênes, and M. Steriade

(1982) Anterograde tracer and field potential analysis of the neocortical layer I projection from nucleus ventralis medialis of the thalamus in cat. Neuroscience *7:* 1861–1877.

Hendry, S. H. C., E. G. Jones, and J. Graham (1979) Thalamic relay nuclei for cerebellar and certain related fiber systems in the cat. J. Comp. Neurol. *185:* 679–714.

Herkenham, M. (1980) Laminar organization of thalamic projections to the rat neocortex. Science *207:* 532–535.

Hobson, J. A., R. W. McCarley, and P. W. Wyzinski (1975) Sleep cycle oscillation: Reciprocal discharge by two brain stem neuronal groups. Science *189:* 55–58.

Hubel, D. H. (1960) Single unit activity in lateral geniculate body and optic tract of unrestrained cats. J. Physiol. (Lond.) *150:* 91–104.

Hyvärinen, J., A. Poranen, and Y. Jokinen (1980) Influence of attentive behavior on neuronal responses to vibration in primary somatosensory cortex of the monkey. J. Neurophysiol. *43:* 870–882.

Inubushi, S., T. Kobayashi, T. Oshima, and S. Torii (1978a) Intracellular recordings from the motor cortex during EEG arousal in unanesthetized brain preparations of the cat. Jpn. J. Physiol. *28:* 669–688.

Inubushi, S., T. Kobayashi, T. Oshima, and S. Torii (1978b) An intracellular analysis of EEG arousal in cat motor cortex. Jpn. J. Physiol. *28:* 689–708.

Itoh, K., and N. Mizuno (1977) Topographical arrangement of thalamocortical neurons in the centrolateral nucleus (CL) of the cat, with special reference to a spino-thalamo-motor cortical path through the CL. Exp. Brain Res. *30:* 471–480.

Jasper, H. H., and J. Tessier (1971) Acetylcholine liberation from cerebral cortex during paradoxical (REM) sleep. Science *172:* 601–602.

Jones, B. E., S. T. Harper, and A. E. Halaris (1977) Effects of locus coeruleus lesions upon cerebral monoamine content, sleep-wakefulness states, and the response to amphetamine in the cat. Brain Res. *124:* 473–496.

Jones, E. G. (1981) Functional subdivision and synaptic organization of the mammalian thalamus. Int. Rev. Physiol. *25:* 173–245.

Jones, E. G., and R. Y. Leavitt (74) Retrograde axonal transport and the demontration of non-specific projections to cerebral cortex and striatum from thalamic intralaminar nuclei in the rat, cat and monkey. J. Comp. Neurol. *154:* 349–378.

Jouvet, M. (1972) The role of monoamines and acetylcholine-containing neurons in the regulation of the sleep-waking cycle. Ergeb. Physiol. Biol. Chem. Exp. Pharmakol. *64:* 166–307.

Kennedy, H., and C. Baleydier (1977) Direct projections from thalamic intralaminar nuclei to extra-striate visual cortex in the cat traced with horseradish peroxidase. Exp. Brain Res. *28:* 133–139.

Klee, M. R., H. D. Lux, and K. Offenloch (1964) Veränderungen der Membranpolarisation und der Erregbarkeit von Zellen der motorischen Rinde Während hochfrequenter Reizung der Formatio Reticularis. Arch. Psychiat. Ges. Neurol. *205:* 237–261.

Krnjević, K. (1981) Transmitters in the motor system. In *Handbook of Physiology*, J. M. Brookhart, V. B. Mountcastle, and V. B. Brooks, eds., Section 1, Vol. II, Part 1, pp. 107–154, American Physiological Society, Bethesda, MD.

Lamarre, Y., M. Filion, and J. P. Cordeau (1971) Neuronal discharges of the ventrolateral nucleus of the thalamus during sleep and wakefulness in the cat. I. Spontaneous activity. Exp. Brain Res. *12:* 488–498.

Livingstone, M. S., and D. H. Hubel (1981) Effects of sleep and arousal on the processing of visual information in the cat. Nature *291:* 554–561.

Llinas, R., and C. A. Terzuolo (1964) Mechanisms of supraspinal actions upon spinal cord activities. Reticular inhibitory mechanisms on alpha-extensor motoneurons. J. Neurophysiol. *27:* 579–591.

Macchi, G., M. Bentivoglio, C. D'Atena, P. Rossini, and E. Tempesta (1977) The cortical projection of the thalamic intralaminar nuclei restudied by means of the HRP retrograde axonal transport. Neurosci. Lett. *4:* 121–126.

Moruzzi, G. (1972) The sleep-waking cycle. Ergeb. Physiol. Biol. Chem. Exp. Pharmakol. *64:* 1–165.

Mountcastle, V. B., R. A. Andersen, and B. C. Motter (1981) The influence of attentive fixation upon the excitability of the light-sensitive neurons of the posterior parietal cortex. J. Neurosci. *1:* 1218–1235.

Mukhametov, L. M., G. Rizzolatti, and A. Seitun (1970) An analysis of the spontaneous activity of lateral geniculate neurons and of optic tract fibers in free moving cats. Arch. Ital. Biol. *108:* 325–347.

Phillis, J. W., and G. K. Kostopoulos (1977) Activation of a noradrenergic pathway from the brain stem to rat cerebral cortex. Gen. Pharmacol. *8:* 207–211.

Purpura, D. P. (1970) Operations and processes in thalamic and synaptically related neural subsystems. In *The Neurosciences: Second Study Program*, F. O. Schmitt, ed., pp. 458–470, The Rockefeller University Press, New York.

Reader, T. A., A. Ferron, L. Descarries, and H. H. Jasper (1979) Modulatory role for biogenic amines in the cerebral cortex. Microiontophoretic studies. Brain Res. *160:* 217–229.

Rivner, M., and J. Sutin (1981) Locus coeruleus modulation of the motor thalamus: Inhibition in nuclei ventralis lateralis and ventralis anterior. Exp. Neurol. *73:* 651–673.

Ropert, N., and M. Steriade (1981) Input-output organization of the midbrain reticular core. J. Neurophysiol. *46:* 17–31.

Sakakura, H. (1968) Spontaneous and evoked unitary activities of cat lateral geniculate neurons in sleep and wakefulness. Jpn. J. Physiol. *18:* 23–42.

Singer, W. (1977) Control of thalamic transmission by corticofugal and ascending reticular pathways in the visual system. Physiol. Rev. *57:* 386–420.

Steriade, M. (1980) State-dependent changes in the activity of rostral reticular and thalamocortical elements. Neurosci. Res. Program Bull. *18:* 83–91.

Steriade, M. (1981) Mechanisms underlying cortical activation: Neuronal organization and properties of the midbrain reticular core and intralaminar thalamic nuclei. In *Brain Mechanisms of Perceptual Awareness and Purposeful Behavior*, O. Pompeiano and C. Ajmone-Marsan, eds., pp. 327–377, Raven Press, New York.

Steriade, M., and M. Demetrescu (1960) Unspecific systems of inhibition and facilitation of potentials evoked in intermittent light. J. Neurophysiol. *23:* 602–617.

Steriade, M., and L. L. Glenn (1982) The neocortical and caudate projections of intralaminar thalamic neurons and their synaptic excitation from the midbrain reticular core. J. Neurophysiol. *48:* 352–371.

Steriade, M., and J. A. Hobson (1976) Neuronal activity during the sleep-waking cycle. Prog. Neurobiol. *6:* 155–376.

Steriade, M., G. Iosif, and V. Apostol (1969) Responsiveness of thalamic and cortical motor relay during arousal and various stages of sleep. J. Neurophysiol. *32:* 251–265.

Steriade, M., V. Apostol, and G. Oakson (1971) Control of unitary activities in cerebellothalamic pathways during wakefulness and synchronized sleep. J. Neurophysiol. *34:* 384–413.

Steriade, M., M. Deschênes, and G. Oakson (1974) Inhibitory processes and interneuronal apparatus in motor cortex during sleep and waking. I. Background firing and responsiveness of pyramidal tract neurons and interneurons. J. Neurophysiol. *37:* 1065–1092.

Steriade, M., G. Oakson, and A. Diallo (1977) Reticular influences on lateralis posterior thalamic neurons. Brain Res. *131:* 55–71.

Appendix 1

Firing rate and interval distribution during wake-sleep states

The numbers in the first column (58-4-28, etc) indicate the cell number: animal-descent-cell. The abbreviations used are: Anti, antidromic; Syn, synaptic; MCx, motor cortex; PCx, parietal cortex; MRF, midbrain reticular formation. In synchronized sleep, a late minor mode is indicated in parentheses.

		Rate	Mode	Percentage of Intervals in Different Millisecond Classes			
				<5	5–100	100–500	>500
		impulses/sec	*msec*		%		
			Waking State				
Group A							
58-4-28	Anti MCx Syn MRF	9.74	37.50	0.94	51.50	43.99	3.57
52-1-11	Anti MCx	7.44	42.50	1.08	44.62	53.12	1.18
44-2-9	Anti MCx	7.55	12.50	9.93	56.29	27.16	6.62
52-2-7	Anti MCx	12.58	12.50	0.66	77.48	21.20	0.66
52-2-8B	Anti MCx	13.16	16.50	3.48	76.31	17.35	2.86
43-2-9	Anti MCx Syn MRF	4.33	3.00	13.40	42.66	26.20	17.74
19-2-10	Anti MCx Syn MRF	5.90	57.50	1.69	46.33	44.92	7.06
15-1-22	Anti MCx	12.92	17.50	0.00	76.19	22.02	1.79
15-1-8B	Anti PCx	8.16	87.50	0.00	72.64	23.59	3.77
18-3-2	Anti PCx	0.76	2.50	10.29	10.40	22.06	57.25
43-2-8	Anti PCx Syn MRF	7.50	17.50	0.00	36.67	20.00	43.33
51-2-7	Anti PCx Syn MRF	7.42	12.50	0.68	62.33	31.74	5.25
19-2-13A	Anti PCx	9.22	9.50	1.69	69.83	22.03	6.45
15-3-9	Anti PCx	5.38	27.50	0.48	61.69	27.71	10.12
			Synchronized Sleep				
Group A							
58-4-28	Anti MCx Syn MRF	6.43	1.75 (210)	57.43	2.92	33.53	6.12
52-1-11	Anti MCx	6.31	1.75	28.48	51.45	20.07	0.00
44-2-9	Anti MCx	4.86	2.25 (130)	24.00	32.20	25.99	17.81
52-2-7	Anti MCx	3.86	1.75 (250)	48.18	13.70	23.74	14.38
52-2-8B	Anti MCx	6.44	2.25 (210)	28.61	43.64	16.82	10.93
43-2-9	Anti MCx Syn MRF	2.70	2.75 (230)	33.33	26.34	21.61	18.72
19-2-10	Anti MCx Syn MRF	3.74	2.25 (90)	27.10	32.58	29.83	10.49
15-1-22	Anti MCx	3.25	2.75 (350)	42.86	19.11	25.48	12.55
15-1-8B	Anti PCx	6.18	62.50	0.42	63.80	28.61	7.17
18-3-2	Anti PCx	2.62	2.25 (390)	56.37	4.14	14.17	25.32
43-2-8	Anti PCx Syn MRF	3.81	2.75 (230)	50.36	9.29	20.71	19.64
51-2-7	Anti PCx Syn MRF	4.33	2.25 (130)	32.48	29.96	24.58	12.98
19-2-13A	Anti PCx	3.57	3.50	9.22	46.60	18.84	25.34
15-3-9	Anti PCx	2.33	1.25 (250)	50.00	5.56	20.00	24.44
			Desynchronized Sleep				
Group A							
58-4-28	Anti MCx Syn MRF	12.90	10.00	21.55	58.49	17.73	2.23
52-1-11	Anti MCx	23.53	3.50	16.02	72.94	11.04	0.00
44-2-9	Anti MCx	8.40	12.50	5.24	67.14	22.86	4.76
52-2-7	Anti MCx	6.16	17.50	4.91	60.38	26.79	7.92
52-2-8B	Anti MCx	13.84	7.50	7.06	75.44	13.81	3.69
43-2-9	Anti MCx Syn MRF	24.16	5.00	21.48	65.32	8.00	5.20
18-3-2	Anti PCx	3.44	2.75	8.06	40.00	33.55	18.39

Appendix 1. Continued.

Firing rate and interval distribution during wake-sleep states

	Rate	Mode	Percentage of Intervals in Different Millisecond Classes			
			<5	5–100	100–500	>500
	impulses/sec	*msec*		%		
			Waking State			
Group B: Syn MRF						
16-4-10A	7.36	7.50	6.79	57.41	29.63	6.17
16-4-13	9.19	12.50	4.21	64.88	27.43	3.48
50-2-13B	14.70	17.50	4.33	75.58	19.32	0.77
50-1-1	20.12	2.50	14.51	72.37	11.53	1.59
15-5-4	13.74	19.50	0.00	82.08	15.68	2.24
18-3-1	1.63	32.50	4.10	18.85	49.18	27.87
18-2-1	9.07	8.50	2.10	47.22	37.48	13.20
15-1-21	5.06	47.50	2.24	26.12	16.42	55.22
15-5-15	3.64	27.50	0.00	45.00	34.17	20.83
15-6-1	3.53	97.50	0.00	32.67	54.67	12.66
16-4-11	12.73	7.50	3.54	73.34	21.58	1.54
19-2-6	11.98	27.50	0.00	79.39	19.59	1.02
			Synchronized Sleep			
Group B: Syn MRF						
16-4-10A	4.90	4.25	11.06	62.98	20.43	5.53
16-4-13	4.47	1.25	21.63	50.85	23.72	3.80
50-2-13B	4.89	1.75	18.70	40.87	28.70	11.73
50-1-1	2.50	1.75 (230)	54.46	10.36	19.44	15.74
15-5-4	6.72	13.50	2.95	79.63	14.32	3.10
18-3-1	2.06	2.75	55.62	10.67	8.54	25.17
18-2-1	2.81	2.25 (390)	58.25	4.56	14.33	22.86
15-1-21	1.90	1.75	55.08	9.38	14.34	21.20
15-5-15	2.59	2.75 (350)	22.67	25.33	26.67	25.33
15-6-1	1.22	2.75 (130)	14.55	14.75	32.73	37.97
16-4-11	2.57	2.75 (230)	24.17	29.66	29.35	16.82
19-2-6	1.10	3.75	19.77	10.47	41.97	27.79
			Desynchronized Sleep			
Group B: Syn MRF						
50-1-1	15.05	2.25	26.45	55.19	15.70	2.66
18-3-1	3.66	22.50	1.56	50.88	30.80	16.76
15-1-21	6.92	27.50	1.19	38.22	20.19	40.40
15-6-1	3.44	62.50	0.00	45.65	41.31	13.04
			Waking State			
Group C: Anti PCx Syn MRF						
17-2-5	65.28	1.25	68.46	30.72	0.77	0.05
17-2-6B	38.28	1.25	16.11	83.24	0.65	0.00
17-2-8	27.65	1.75	27.22	66.80	5.66	0.32
17-2-4	66.78	1.15	82.64	12.97	4.32	0.07
			Synchronized Sleep			
Group C: Anti PCx Syn MRF						
17-2-5	38.25	0.95	69.69	20.80	7.98	1.53
17-2-6B	26.35	1.05	56.80	28.65	11.32	3.23
17-2-8	7.38	1.25	79.19	4.75	9.73	6.33
17-2-4	41.61	1.05	86.95	5.49	6.87	0.69
			Desynchronized Sleep			
Group C: Anti PCx Syn MRF						
17-2-5	30.32	1.05	34.08	58.51	6.04	1.37
17-2-8	31.20	1.75	56.07	34.51	9.10	0.32
17-2-4	29.68	1.25	63.07	22.10	14.83	0.00

Appendix 2

Antidromic responsiveness in wake-sleep states

These are percentage values of antidromically elicited discharges in a group of 19 cortically projecting (MCx, motor cortex; PCx, parietal cortex) CL-Pc neurons during wakefulness (W) and synchronized sleep (S); 5 of them also were tested during desynchronized sleep (D).

Cell Number	Stimulated Site	Latency	W	S	D
52-1-13	MCx	1.2	80	64	96
52-1-11[a]	MCx	1.3	90	65	
19-2-14	MCx	1.6	35	12	
52-1-6	MCx	1.8	100	52	
52-2-7[a]	MCx	1.8	100	55	
52-2-8B[a]	MCx	1.8	100	68	
19-1-11	MCx	2.0	100	30	
15-5-16	MCx	3.0	44	16	52
19-2-10[a]	MCx	3.9	95	62	
17-2-5[a]	PCx	0.3	96	83	
17-2-8[a]	PCx	0.4	72	4	100
17-2-4[a]	PCx	0.5	45	31	40
15-1-8B[a]	PCx	1.3	90	90	
19-2-4	PCx	1.5	90	72	
18-3-2[a]	PCx	1.5	100	62	100
51-2-7[a]	PCx	1.8	80	0[b]	
19-2-13A[a]	PCx	3.0	58	56	
15-3-9[a]	PCx	3.4	80	38	
19-2-5	PCx	4.5	100	75	

[a] Neurons whose spontaneous firing could be recorded in another sleep-waking cycle without testing shocks (see their discharge rates in Appendix 1).

[b] This refers to the neuron depicted in Figure 8*A* which discharged only IS spikes to antidromic volleys during S (the values of all neurons are calculated for full IS-SD spikes).

Steriade, M., G. Oakson, and N. Ropert (1982) Firing rates and patterns of midbrain reticular neurons during steady and transitional states of the sleep-waking cycle. Exp. Brain Res. *46:* 37–51.

Stone, T. W., D. A. Taylor, and F. E. Bloom (1975) Cyclic AMP and cyclic GMP may mediate opposite neuronal responses in the rat cerebral cortex. Science *187:* 845–847.